45th AIAA Aerospace Sciences Meeting and Exhibit
8 - 11 January 2007, Reno, Nevada

AIAA 2007-776

Simulation of Nozzle Erosion Process in a Solid Propellant Rocket Motor

Nicholas D. Liggett[1] and Suresh Menon[2]
The Georgia Institute of Technology, Atlanta, GA 30332-0150

This paper presents an approach to the simulation of erosion within a rocket nozzle from fundamental principles that relies on as little empirical data as possible. A model is developed that accounts for shear and pressure forces, particle impacts, heat transfer and its subsequent diffusion through the nozzle material, and surface chemical kinetics. The model is based on macro-scale dynamical model concepts, which allow the particle impacts to be modeled based on a lattice method and properties of the material. The macro-scale dynamical model is extended by solving the energy equation at each lattice point for thermal effects, applying surface forces to surface site, and applying chemical kinetics to surface sites. The thermal model, chemical model, and surface regression are validated against experiments and other simulations, and they are all found to be accurate in the subgrid scales that are to be modeled. The chemical erosion of a carbon nozzle in an H_2O-CO_2 environment over a range of pressures and compositions is studied, and high erosion rates are seen for flows with high water content at high pressures. Additionally, preliminary erosion studies are performed on niobium and tungsten-rhenium materials. It is found as expected that the more ductile and lighter niobium is subject to more erosion by particle impacts. Niobium is found to be subjected to significant erosion by particle impacts and thermal effects, whereas erosion of tungsten-rhenium is found to be almost entirely due to thermal effects in a nozzle-like environment. The model has been developed enough that it is ready for full integration into internal rocket flow field solvers.

I. Introduction

THE erosion of the walls of a solid rocket nozzle is caused by various physical factors. Most notable factors among them are erosion due to thermo-fluid characteristics like heat transfer to the walls, shear and normal stresses, turbulence in the flow, temperature, pressure, surface chemical reactions and particles impinging on the nozzle walls.[1] These effects are diagrammed in Fig. 1. The erosion near or at the nozzle wall is of particular interest here since the throat of a solid propellant rocket nozzle is subject to extreme conditions.[2] It is the region of the highest heat transfer, and this extreme heat transfer along with surface shear forces and impact of particulates in the flow can lead to surface erosion of the nozzle and a change in its characteristic. Two failure modes might occur. Either the rocket might fail catastrophically as the throat weakens, or the throat might grow to the point where the flow is no longer choked. Either case is undesirable, and therefore understanding of throat erosion is critical to design. Additionally, to increase the performance of rockets, it is desirable to increase the chamber pressure. This increase leads to even more intense conditions at the throat. A fundamental understanding of the underlying processes is not currently available since it is nearly impossible to fully resolve the processes occurring near the wall. Current erosion prediction methods are either highly specific or lacking all aspects of the nozzle erosion process.[3-9] As such, the need for better understanding of throat erosion from a more fundamental viewpoint and its sensitivity to chamber operating conditions is even more apparent.

The current study is focused on developing a comprehensive simulation strategy that can capture not only the local thermo-chemical processes impacting nozzle erosion but also the geometrical changes to the nozzle surface. To accomplish this we need a simulation approach that includes both the physics of the processes and the ability to capture the changes to the geometry of the nozzle surface in response to these processes. An added difficulty is that

[1] Graduate Research Assistant, Computational Combustion Laboratory, School of Aerospace Engineering; Nicholas.Liggett@gatech.edu. Member AIAA.
[2] Professor, Director, Computational Combustion Laboratory, School of Aerospace Engineering; suresh.menon@gatech.edu. Associate Fellow AIAA.

the heat transfer, chemistry, and mechanical time scales of erosion are all very different creating a still system to solve. These fine-scale physics have to be captured within a simulation framework that also resolves the gas phase combustion physics that constitute the prescribed conditions under which the erosion takes place.

Current erosion simulation strategies focus one only one or two aspects of the erosion process or they cannot be generalized to suit the needs of nozzle erosion. Much erosion work has been devoted to the prediction of gun barrel erosion;[3,4] however, this work is highly specific to the situation of gun barrel erosion and difficult to apply to nozzle erosion. Another erosion model that is designed to simulate erosion due to dilute particle impacts[5,6] agrees well with experiments, but it contains only the effects of particle impacts and is not easily extensible to include all erosive effects along with a moving wall boundary. It also relies on knowing empirical parameters, such as the area of contact between the particles and the boundary, which may not be known a priori for high speed impacting particles, which can deform and break apart upon impact. Erosion models that are specifically tailored to predict erosion in a solid rocket motor due to alumina particles also exist.[7] This model also includes the effects of heat transfer to the surface. Unfortunately it does not fully account for surface kinetics and relies on empirical parameters for the particle impact model, restricting its use. Finally, models that are focused on ablation of protective linings[8,9] sufficiently account for heat transfer, but they lump together all chemistry that occurs at the surface or rely on correlative equations, so that understanding the workings of the aspects of erosion is difficult.

This study aims to create a comprehensive erosion model that can account for all aspects of the erosion process within a rocket nozzle. We seek to create an erosion model that not only correctly predicts erosion, but is based on first principles, so that the erosion process is not hidden behind empirical relations. Many hot gas flows contain aluminum, unburned solid fuel chunks, or other particles that may impact the nozzle surface mechanically eroding it. The impacting of these particles is difficult to model, so we start with a model that can effectively predict erosion due to particle impacts. The basic approach is derived from the current macro-scale dynamic (MSD) model, which has been developed and validated by other authors.[10-12] This model was specifically designed to model erosion due to these particle impacts. It is based on first principles of Newton's laws of motion applied to a discrete lattice representing the surface, and as such is applicable to almost any situation involving particle impacts. This approach provides an excellent framework, in that it is extensible (properties can be added to the lattice points as desired) and allows materials that are nonuniform in composition and even composite materials to be analyzed.[13] Additionally, the model allows simulation at the scale at which erosion takes places without being prohibitively slow for computations, as an atomic model would be. The MSD model as created by other authors is lacking for our purposes, in that it includes no allowances for heat transfer or chemical kinetics. The MSD model models particle impacts well, but it must be extended to include all aspects of nozzle erosion.

Our previous work[1,14] was developed from this macro-scale dynamical model; however, our work included only surface forces, particle impacts and some heat transfer effects. The model as we have currently developed it has further included chemical kinetics and full coupling between all different erosion aspects. Additionally, our current model has been used to perform initial erosion studies in a rocket nozzle. The erosion model that is developed includes the effects of pressure and shear forces. Heat transfer effects are also included, as they are known to lead to melting of the material and thus erosion of the nozzle.[9] Numerical heat transfer models, which are well established understood,[15,16] are quickly and easily developed to fit into the framework of the MSD model. Although it is not included in this study, the effect of thermal expansion can be added. The heat transfer model is coupled to the MSD model by considering the altering of thermo-chemical properties of the nozzle due to temperature variation. Heat transfer leads not only to melting of the material, but the increase in temperature weakens the nozzle mechanically and increases the reaction rates of heterogeneous reactions occurring at the nozzle surface.[17] These heterogeneous reactions are another source of nozzle erosion that is included in the study, as they can be a significant source of erosion in carbon nozzles.[18] A chemical model based on Surface Chemkin for predicting the heterogeneous reaction rates at a gas-solid interface is also utilized.[19-21] Surface Chemkin is an extremely rich package that can do much more than is necessary for the nozzle erosion process as modeled by us. As such, a much simpler chemical model is created by utilizing the concepts of Surface Chemkin. Finally, in order to truly capture the erosion process the fully developed model will be coupled to a LES based solver developed by other authors.[22]

The rest of the paper is organized into the model formulation, numerical implementation, results and discussion, and conclusion sections. In the model formulation the details of the physics of each of the aspects of the erosion process are considered. The MSD model is also explained in detail. In the numerical implementation section, the validations of the heat transfer, surface regression, and chemical kinetics aspects of the model are discussed. All pertinent inputs to the simulations are given and the data used for validation are discussed. The setup for the erosion studies is also given. In the results and discussion section the results of the validation simulations are compared to the expectations from classical analyses and other studies. The results of the nozzle erosion studies are also given and analyzed to understand the different responses of the different materials.

II. Model Formulation

In the MSD model the target material and the impacting particle(s) (if applicable) are discretized onto a lattice. Each site of the lattice represents a small fictitious volume of the material. During the erosion process, any lattice site is vulnerable to movement due to the action of the external forces caused by various processes such as surface chemistry, surface shear and normal loads, as well as due to interactions between any pair of adjacent sites. Each pair of adjacent sites is linked by an imaginary "bond." This bond should not be mistaken for a molecular bond between a pair of atoms, but as a hypothetical bond for the purpose of modeling. The deformation of this imaginary bond is responsible for the interactions between any pair of adjacent sites. This deformation is, in turn, dependent on the mechanical properties of the material. Any bond between two adjacent sites will break if the mechanical strain caused in the bond due to its deformation exceeds the fracture strain of the material. Any site or a group of sites is liable to be eroded away if all the bonds surrounding it are broken due to fracture.

The erosion model simulates the processes that occur not only on the surface of the nozzle wall but also the processes that occur within the nozzle material. For example, due to surface chemistry, shear forces and/or particle impacts the sites at the top of the material can become displaced. This displacement can cause their immediate neighbors to also become displaced. This process is carried on to other sites all throughout the material, thereby resulting in wear in the material. Heat transfer from the gas phase to the wall also propagates through the material and impacts the local thermo-mechanical properties of the material at each of the lattice points.

The MSD model is implemented within a finite volume approach that is well suited to a grid in which pieces are removed by erosion. An interior site of the nozzle wall is seen in Fig. 2a. The springs represent the forces between the site and its neighboring sites. Heat transfer also occurs along these springs. The state and change in state of an interior node is dependent upon only initial conditions and its neighboring nodes; however, for an exterior node, boundary conditions such as prescribed heat transfer or temperature are applied.

An example of an exterior site is shown in Fig. 2b, where the bond between node and its top neighbor does not exist, so that no conductive heat or force transfer can occur. At this surface site, shear forces can be seen that are dependent on the shear stress at the surface. There will also be pressure forces that are not shown for clarity. Finally, this surface site will have mass loss from its point mass load due to chemical kinetics. If this surface site is removed by erosion the site below it will become a surface node.

The total force on any particular site is due to the external force, as well as due to interaction between any pair of adjacent sites. For homogeneous materials, the force of interaction between a pair of adjacent sites can be expressed as: $f = k\Delta l$, where k is a force coefficient, which is dependent on the Young's modulus (E), yield strength (σ_y) and tensile strength (σ_T). Here, Δl represents the deformation of a bond between a pair of adjacent sites. The value of k depends on whether the current strain in the bond is in the elastic or plastic region. The elastic region is linear by Hooke's law, and the plastic region is approximated to be linear in the present model (this approximation can be relaxed later). The value of k is equal to E_eA/l_o, where E_e is the elastic modulus, A is the contact area between the adjacent sites, and l_o is the initial bond length under un-deformed state. In the plastic region, the value of k is given by E_pA/l_o where E_p is the stress to strain ratio in the plastic region as shown in Fig. 3. The value of E_p is equal to $(\sigma_T - \sigma_y)/(\varepsilon_T - \varepsilon_y)$, where ε denotes the corresponding strains. The material is assumed to be isotropic at present, and therefore, the orientation of the deformed bond does not change the value of k, and hence the magnitude of the bond force. The total force on any site (e.g. site p) on the surface of the material is given by:

$$\vec{F}_p = \sum_q^n k\Delta\vec{l}(p,q) + \vec{f}_p \tag{1}$$

where n is the number of sites q adjacent to site p and f_p is the external force as a result of surface shear and normal stresses. The value of n depends on the location of the site p. For example, in 2D, if p is an interior point then $n = 4$. If it is an edge point then $n = 3$ and if it is a corner point $n = 2$. The x-displacement can also cause a y-force on a site and vice versa. This is accounted by the Poisson's ratio, v. The deformation vector of the bond between any two adjacent sites p and q is given by:

$$\Delta\vec{l}(p,q) = \vec{l}(p,q) - \vec{l}_o(p,q) = \left[\vec{r}(q) - \vec{r}(p)\right] - \vec{l}_o(p,q) \tag{2}$$

The external force f_p exists only for a site on the top surface of the material exposed to shear and pressure forces. These shear and pressure forces are prescribed from the solution of the flow in the nozzle given by a flow field

solver. Thus, knowing the force on a site at time t, the velocity and position of the site at a time $t + \Delta t$ can be determined from the following equations:

$$v_{t+\Delta t}(p) = v_t(p) + \frac{1}{m} F_t(p)\Delta t \tag{3}$$

$$r_{t+\Delta t}(p) = r_t(p) + v_t(p)\Delta t \tag{4}$$

Thus, using the above equations, the velocities and positions of each site can be predicted for different time steps from which the force can be calculated. The mechanical strain caused in any bond can be denoted by: $\varepsilon = \Delta l / l_o$. If the strain is less than the elastic limit ε_y, the displacement of a site is recoverable. If the strain is within the plastic limit ($\varepsilon_y < \varepsilon < \varepsilon_T$), a plastic deformation occurs to the bond, resulting in a permanent displacement even upon removal of the external load. Under these circumstances, the length of the stress-free bond (l_o) changes to a different value given by:

$$l_o^* = l_o\left(1 + \Delta\varepsilon_p\right) \tag{5}$$

where the residual strain is given by: $\Delta\varepsilon_p = \Delta l / l_o - \varepsilon_y$.

As mentioned earlier, if the strain ε exceeds the fracture strain ε_f, the bond will break. Erosion of a site or a group of sites is caused when all the bonds surrounding it are broken. Upon transferring the forces from the impacting particle to the material sites, the velocities and positions of the sites can be calculated at the next time step and this procedure is repeated, thus simulating wear of the material due to particle impact.

Chemical heterogeneous reactions on the nozzle surface are also included in the current formulation. In particular, we consider the reactions of carbon surface material with H_2O and CO_2 in the current study, and the pyrolysis of pure ammonium perchlorate. Any chemical mechanism can be utilized in the model provided the heterogeneous reaction rates are known. Overall, these kinetics are modeled using modified Arrhenius rate equations of the form $k = AT^{\eta}\exp[E_A/(RT)]$, where A, η, and E_A are empirical constants that are different for each reaction of the mechanism. The mass removal rate at the nozzle surface is then given by the reaction rate and may also have a pressure dependence term for the reacting gas components. No internal nodes are affected by chemistry, as they have no exposed surface area that can react. Surface reactions result in mass removal from the nozzle wall and also result in surface regression. This effect is explicitly included within the MSD model.

Note that this model does not explicitly alter the composition at the surface of the nozzle wall. The model instead has a prescribed composition and state at the surface as given by a flow field solver. The prescribed composition is used to find reaction rates and in turn mass removal rates. The total mass and its composition are then treated as output from the model. In order to then inject the eroded mass into the nozzle flow this model must be coupled to a flow field solver. This coupling to a flow field solver is one of the future goals of this study.

Additionally, thermal effects are included in the model. Each site is subjected to the conservation of energy in integral form as follows.

$$\frac{d}{dt}\int_V e\rho \, dV = \int_A \dot{q}''_{\text{heat}} dA + \int_V \dot{q}'''_{\text{prod}} dV \tag{6}$$

Here, e is the mass specific internal energy and ρ is the density of the site. The left-hand side of the energy conversation equation is the rate of change of the total energy at the site, where the integral is over the volume of the site. The first term on right-hand side is the diffusion of energy through the boundaries of the site, where the integral is over the surfaces of the site. The second term on the right-hand side is the volume specific energy production rate. The energy is related to the temperature by $e = c_p T$, where c_p is the specific heat capacity and T is the temperature of the site. The diffusion of energy through the boundaries is given by Fourier's law of conduction, using the thermal conductivity at the site. Energy can be released or consumed through chemical reactions at the surface sites. A site will be eroded and removed from the material matrix if it reaches the melting temperature of the material. Note that energy transfer by radiation is not included in Eq. (6).

The thermal model must also be coupled to a flow field solver. For one-way coupling, the thermal model can take the solution from the solver (i.e. wall temperature or wall heat flux) as input. The thermal model is then coupled back to the flow field solver through the sensible enthalpy of the products and by determining the temperature profile through the nozzle wall.

Once the nozzle erosion model is completely integrated into the flow field solver, seamless erosion calculations can be performed. The unsteady flow within a rocket nozzle will be determined. After a given number of integration time steps of the flow field solver, the erosion model will then be utilized at the subgrid scale. The flow information (wall temperature, composition at the nozzle wall, etc.) will be used as input for the nozzle erosion model. The nozzle erosion model will then be run between time steps along the nozzle wall. Its output (composition and mass injected into the flow, new wall shape, etc.) will be used to modify the boundary conditions of the flow field solver for the next set of integration time steps.

III. Numerical Implementation

Validation simulations were performed for each aspect of the model individually. For the thermal model validation, the thermal response for a 2 mm by 1mm (x by y) section of pure ammonium perchlorate was simulated. This grid is representative of the order of the size of a sub-grid that will be used in future nozzle erosion studies. The properties used for ammonium perchlorate are a density (ρ) of 1760.0 kg/m^3, thermal conductivity (k) of 0.4114 W/m/K, specific heat capacity (c_p) of 1593.6 J/kg/K, and melting temperature (T_M) of 825.0 K[23,24]. No chemical kinetics, shear or pressure forces, or particle impacts were considered for the thermal model validation. Simulations were performed lasting 1.0 s with an integration time step of 0.2 ms. The wall began with an initial temperature profile as given by:

$$T(x,y) = T_{\max}\left(\frac{x}{a}\right)\left(\frac{y}{b}\right) \tag{7}$$

where a and b, the extents of the domain, were 2 mm and 1 mm, respectively, and T_{max} was 800 K. The boundary conditions for all boundaries were isothermal with all walls held at 0 K. Simulations were performed with uniform grids consisting of a constant 101 nodes in the x-direction by 11 through 101 nodes in the y-direction at 10 node increments. Grid spacing was chosen so as to produce simulation results that were independent of the grid without having too many extra nodes.

The results were compared to the classical exact analytical solution for this problem as shown in Eq. (8),[25] where k is the thermal conductivity as given in Table I. The infinite series was truncated at 400 terms for both m and n.

$$T(x,y,t) = \frac{4\cdot a\cdot b}{\pi^2}\sum_{m=1}^{\infty}\sum_{n=1}^{\infty}\frac{(-1)^{m+n}}{m\cdot n}\cdot\sin\left(\frac{m\cdot\pi\cdot x}{a}\right)\cdot\sin\left(\frac{n\cdot\pi\cdot y}{b}\right)\cdot\exp\left[\frac{\left(m^2+4\cdot n^2\right)\cdot\pi^2\cdot k\cdot t}{a^2}\right] \tag{8}$$

With the thermal model validation completed, validation simulations were also performed for the surface regression model, using the pyrolysis of ammonium perchlorate, which has been extensively studied.[23,24] This pyrolysis was assumed to occur by a single step mechanism from condensed phase to gaseous phase with Arrhenius reaction rate parameters $A = 5.0\cdot10^6$ kg/m^2/s, $\eta = 0.0$, and $E_A = 92{,}109.6$ J/mol. The domain was 2 mm by 1 mm, with a uniform grid having 101 nodes by 101 nodes. The boundary conditions were adiabatic at for the left and right boundaries, second-order accurate extrapolation for the bottom boundary, and adiabatic for the top boundary, which was the reacting surface. The melting temperature and thermal properties used are given in Table I.[23,24] The surface regression model was validated by considering the chemistry separate from the thermal model, and as such no heat release was considered during surface regression validation. Surface regression rates were determined with uniform initial temperatures ranging from 700 K to 820 K, a temperature range of fast kinetics without melting, for the pure ammonium perchlorate simulations. The simulation time was 0.3 s with an integration time step of 0.2 ms, where the time step was chosen based on stability concerns.

The exact surface regression rate expected with no heat release as calculated using the pyrolysis reaction rate is the given by Eq. (9), which is used for verification of the surface regression model, where ρ_{AP} is the density of ammonium perchlorate from Table I and the other parameters are from Table II.

$$\dot{r} = \frac{A}{\rho_{\mathrm{AP}}} \exp\left(\frac{E_{\mathrm{A}}}{RT}\right) \tag{9}$$

The chemical model was also validated by considering the erosion of a graphitic carbon surface in a H_2O-CO_2 hot gas flow as has been studied by other authors.[26,27] The thermo-mechanical properties of carbon used are a density of 2267.0 kg/m^3, thermal conductivity of 140.0 W/m/K, specific heat capacity of 710.2 J/kg/K, and melting temperature of 3800.0 K.[28] The heterogeneous reaction mechanism considered is as follows:[18]

$$\mathrm{C(s) + H_2O(g) \rightarrow CO(g) + H_2(g)}$$

$$\mathrm{C(s) + CO_2(g) \rightarrow 2CO(g)} \tag{10}$$

The reaction rates corresponding used for the mechanism are given in Table I. [26,27] The recession rate of the carbon nozzle was determined for a range of pressures from 1000 psi to 9000 psi with the composition of the hot gases varying from pure water to pure carbon-dioxide. The nozzle wall domain was 4 mm thick and 2 mm long with 2 nodes long by 171 nodes into the wall. Again, the number of nodes in the *y*-direction was chosen as near the smallest value that maintained a grid-independent erosion rate. A one-dimensional setup was used, as the recession rate was desired with only uniform surface properties. A review of the literature gave an average throat nozzle wall temperature of 2500 K, so an isothermal wall boundary condition of 2500 K was used. Adiabatic boundary conditions on the left and right walls were used and a second-order extrapolation boundary condition for the bottom boundary was used. The initial wall temperature was uniform at 300 K, a cool nozzle that will be heated by the flow. The simulations were run for 1.0 s with time steps of 8μs, with the time step being chosen to maintain stability. Due to the much larger thermal conductivity of carbon as compared to ammonium perchlorate, a smaller time step was necessary for stability concerns. The simulations were compared to existing data for validation.[29,30]

Table I. Reaction rate parameters for graphitic carbon reduction.

Reactant	Pre-exponential factor, A, $kg_C/m^2/s/atm^{0.5}$	Temperature exponential, η	Activation energy, E_A, kJ/mol
H_2O	$4.80 \cdot 10^5$	0.0	287.9
CO_2	$9.00 \cdot 10^3$	0.0	284.9

Finally, erosion studies were performed using the MSD model on a variety of materials to ascertain the qualitative effects of the aspects of erosion. Particle impact and heat transfer simulation were performed on tungsten-rhenium (25%-75%) and niobium nozzles. The mechanical properties used for these materials are given in Table II, and the thermal properties are given in Table III. For the impacting particles, aluminum was used. Its mechanical properties are also given in Table II.

Table II. Mechanical material properties for nozzle wall for simulation.

Material	Density, ρ, kg/m^3	Elastic modulus, E, GPa	Yield strength, σ_y, MPa	Fracture strength, σ_f, MPa	Fracture strain, ε_f
Niobium	8570	103.0	105.0	195.0	0.30
Tungsten-rhenium	16693	430.0	1524.0	1627.0	0.11
Aluminum	2713	69.0	34.5	89.6	0.35

Table III. Thermal material properties for nozzle wall for simulation.

Material	Melting point, T_M, K	Specific heat capacity, c_p, J/kg/K	Thermal conductivity, k, W/m/K
Niobium	2740	265.0	54
Tungsten-rhenium	3373	137.8	30

Large-eddy simulations were performed using a Runge-Kutta solver[22] on a nozzle and the results were used as input for the erosion studies. Subgrid simulations were performed at three stations in a nozzle: one located just before, one located at and one located just after the nozzle throat. These simulations include particle impacts, heat

transfer and shear force effects. The nozzle wall subgrid had 50 by 20 nodes, whereas the aluminum particles had 8 by 8 nodes. The grid spacing was chosen so that the erosion solution was grid independent, without wasting computational power on too many grid nodes. The size of the subgrid was 1 mm across with varying height around 0.4 mm. The particle size was 16 μm squared. Particle size and amount by volume was determined from Atlas solid rocket motor measurements.[31]

IV. Results and Discussion

In order to ascertain the accuracy of the thermal model, the results obtained from the variable grid spacing were compared to the exact analytical solution. The RMS error between the numerical solution and the analytical solution were calculated for the grid spacing that varied in the *y*-direction. The results are given in Fig. 4a, where the points give the RMS error of the simulations. The *x*-axis is grid spacing, which is proportional to the inverse of the number of grid nodes; therefore, the data points are inversely spaced on the *x*-axis. A quadratic curve has also been fit to the data with a forced y-intercept at 0 K. The excellent fit of this quadratic curve demonstrates the thermal model does indeed have second-order accuracy. Deviation from the second-order accuracy could be attributed to error in calculating the analytical solution. The double infinite series converges slowly, so that even with 160,000 terms, measurable error was still present. The maximum temperature in the domain was 55 K, so that with only 11 nodes in the *y*-direction, the RMS error was 1% of the maximum temperature. As noted previously the thermal model validation simulations were run for 1.0 s. The accuracy of the model at 1.0 s ensures the model will be accurate for the smaller time-scales of the sub-grid nozzle erosion model. The accuracy of the thermal model has been demonstrated.

Shortcomings still exist in the thermal model, which are not considered here. Heat transfer by radiation is not considered in the model at current, and this can account for up to 35% of the heat transfer at the nozzle wall surface. Additionally, thermal expansion can be added, which will further couple the force model to the thermal model.

The surface regression results are considered next. The surface regression rate simulation data as a function of temperature for the pure ammonium perchlorate simulations is plotted in Fig. 4b as symbols. The expected regression rate as given by Eq. (9) is also plotted as a solid line. The surface regression rate varies exponentially with temperature as expected due to the exponential dependence of the pyrolysis rate on temperature. The simulated surface regression rate varies from the expected value by at most 7.9% at 700 K. The error is due to the discrete nature of the finite-volume formulation of the problem, so that the erosion surface can lie only at a finite number of points in the *y*-direction. Additionally, if a cell is eroded, there is additional pyrolysis loss for the newly exposed that is not accounted for during the same integration time step; however, this last source of error is minimized by utilizing a grid that is fine enough to produce grid-independent solutions.

The chemical model validation consisting of heterogeneous combustion of carbon gave nozzle recession rates as seen in Fig. 5. The recession rate of the carbon nozzle is plotted as a function of the percent of the hot gases that are comprised of water. The rest of the hot gases were carbon-dioxide. The different curves represent different chamber pressures of the rocket (not throat pressures). As expected the nozzle erosion rate increases with increasing pressure. The pressure jump from 1000 psi to 2000 psi gives more nozzle erosion than the same jump from 2000 psi to 3000 psi. This occurs because there is a quadratic dependence on pressure that arises from the dependence of both reaction rates on the roots of the partial pressures of water and carbon dioxide

Due to boundary conditions the melting point of carbon was never reached during the simulation, and as such all erosion was due to chemical kinetics. A realistic nozzle environment might have a chamber pressure of 1000 psi and a water content of 43%. This corresponds to a recession rate of 0.86 mm/s in Fig. 5. This prediction agrees well with published experiments of graphitic nozzle erosion in actual rocket nozzles.[30] In Fig. 5 the erosion rate increases with increasing water content. The erosion rate is not zero at 100% carbon-dioxide, but it is still very small. Apparent in Fig. 5 is that the erosion rates can reach several mm/s so that some kind of erosion mitigation technique must be employed. Erosion mitigation might be obtained by reducing the water content of the exhaust, or creating a thin film of CO_2 (for this situation) on the surface of the graphite. Note that this study does not include diffusion limited erosion; however, once the erosion model is fully coupled to the flow field solver the effects of diffusion will be inherently included. Also, due to the exponential dependence on temperature, the chemistry is extremely sensitive to the temperature at the surface of the nozzle. Care must be taken in coupling the erosion model to the flow field solver so that the temperature at the nozzle surface is calculated correctly.

A profile of the rocket nozzle simulated for the erosion studies is shown in Fig. 4a. The boxed area is the area of interest for the erosion studies. This area can be seen in close-up in Fig. 4b. The three boxed areas in Fig. 4b are the three stations at which the detailed erosion simulations were carried out. The pertinent results for the simulation of the rocket nozzle are given in Table IV for three stations, before, at, and after the throat.

Table IV. Results from the nozzle simulation used for erosion studies.

Station	Position, mm	Particle velocity, m/s	Wall shear, kPa	Wall heat transfer, kW/m^2
1	**171.56 (before throat)**	**613.4**	**61.7**	**134.7**
2	**173.75 (at throat)**	**876.6**	**116.9**	**145.7**
3	**181.51 (after throat)**	**1193.1**	**55.5**	**108.7**

Results for the erosion simulations are found in Figs. 5 through 7. Note these figures correspond to the dashed boxes in Fig. 4b. The impacting particles in Figs. 5 through 7 come from the bottom of the figure upward to the material lattice at the top. A total of 44 particle impacts occur during the simulation. The tungsten-rhenium material is a representative material often seen in rocket nozzles. The niobium material is a reference refractory metal. It is apparent in the figures that erosion before and at the throat is much worse than after the throat. This is likely due to particle impacts have a much high angle of before the throat than after it. In Fig. 7 it is apparent that the erosion is much more widespread, but it is also much shallower. Low particle impact angles cause glancing blows on the wall material that might couple with thermal erosion to produce the widespread, shallow erosion. Apparent in all figures is the level that the tungsten-rhenium nozzle stands up to the erosion compared to the niobium nozzle. The niobium was eroded at an average rate of 0.02 mm/s before and at the throat, whereas it was eroded at an average rate of 0.01 mm/s after the throat. The tungsten-rhenium nozzle was eroded at 0.002 mm/s, an order of magnitude less erosion than the niobium. The reduced erosion as compared with other refractory metals makes the reasoning for using it in rocket nozzles clear.

Figures 8a and 8b show the results of the simulation with heat transfer effects only considered. Particle impacts are removed in this portion of the simulation in order to isolate the effects of heat transfer. The total simulation time for this simulation is 0.5 s. Shear force effects were found to have no visible effect on the results if they were off or on. Shear force effects would likely increase in importance if a melt wipe layer were added.

Both materials are nearly uniform in temperature due to the thinness of the nozzle wall and high thermal conductivity of the metals. The differing melting paths of the two materials are visible in the diagrams. The niobium melting path is deeper, whereas the tungsten-rhenium melting path is wider. The niobium has thermal conductivity nearly twice that of the tungsten-rhenium, meaning the heat penetrates deeper into the material. Also, although the tungsten-rhenium has a lowed heat capacity, it has a much higher density and higher melting point than the niobium. It takes much more energy transfer for the tungsten-rhenium to heat to melting, so the melting path is not as deep. Melting begins at the right side because the heat transfer rate imposed by the LES results is higher on that side. The niobium nozzle had an average erosion rate of 0.46 mm/s as compared with the tungsten-rhenium nozzle erosion rate of 0.40 mm/s. Again, the lower erosion rate of tungsten-rhenium supports its use as a rocket nozzle material.

The tungsten-rhenium nozzle is seen to be completely limited by thermal erosion, as compared to the niobium nozzle, which has strong erosion due to both thermal and particle effects. It is clear that the relative importance of erosion aspects is different between even similar refractory metals due to differing thermo-mechanical properties. The erosion mitigation solution for tungsten-rhenium would involve perhaps only some cooling mechanism (e.g. a cooling gas injection layer), whereas a solution for niobium would be more complex (e.g. perhaps including both a cooling gas injection layer and coating to protect it from particle impacts).

V. Conclusion

The primary objective of the study is to develop a comprehensive model that can simulate the erosion process in a rocket nozzle, predict erosion rates and paths for future, high pressure nozzles, and allow a greater understanding so that erosion mitigation methods can be developed. The primary aspects of erosion to be completed were determined to be surface forces, particle impacts, heat transfer, chemical kinetics, and surface melting. A MSD node centered, finite-volume model formulation was extended from being having only particle impact effects, to also include shear and pressure forces, heat transfer, and chemical kinetics.

This model was validated independently from any flow field considerations. Thermal validations were performed that found the temperature profile within a specimen of pure ammonium perchlorate subject to isothermal boundary conditions and a given initial temperature profile over a range of grid sizes. When the simulations were compared to the exact analytical solution, the spatial second-order accuracy of the formulation was shown. A maximum error of about 1% was seen with a grid having 11 nodes in the y-direction. The inherent surface regression aspects of the MSD model were also validated by considering the regression of the ammonium perchlorate specimen under with an initial temperature varying from 690 K to 810K. No heat of pyrolysis was used, as the surface regression model independent of heat transfer was being validated. The error between expected regression rate and

actual regression rate was between 2.4% and 7.9% for the temperature range, due to discretization in the grid. This error was reduced when grid resolution was improved. Finally, the chemical kinetics of the model was validated by considering the case of carbon nozzle erosion due to the flow of hot H_2O-CO_2 gases. The carbon was found to recess at 0.86 mm/s for a realistic nozzle environment with a chamber pressure of 1000 psi and water content of 43%, which is in line with expectations for a carbon specimen in a hot nozzle environment.

Erosion studies were performed on tungsten-rhenium (25%W/75%) and niobium nozzles at stations before, at, and after the throat using data from LES work. As expected, the tungsten-rhenium nozzle faired better again impacting particles. The more ductile and weaker niobium was subjected to an order of magnitude deeper and more widespread erosion due to particle impacts. Additionally, the niobium nozzle suffered slightly deeper erosion due to its lower overall heat capacity. In the case of niobium, heat transfer and particle impacts were seen to have about equal importance, whereas for the case of tungsten-rhenium heat transfer was the clearly dominating factor.

Future studies will form a two-way coupling between the erosion model developed here and the flow field solver, so that time-dependent erosion effects can be ascertained. The surface kinetics of tungsten-rhenium will be ascertained so that erosion studies can be performed that include all erosive effects on multiple real-world nozzle materials. Additionally, if liquid melt layer effects are determined to be important, they will be added to the erosion model. From there, parametric studies of erosion can be performed to allow the relative importance of each aspect of erosion to be determined.

Acknowledgments

This work was funded by a subcontract from Penn State University under an Office of Naval Research (Dr. Judah Goldwasser, Program Manager) MURI on "Fundamental Understanding of Propellant/Nozzle Interaction for Rocket Nozzle Erosion Minimization under very High Pressure Conditions".

References

[1]Hanagud, Sathya V., Wilkinson, Angus, Menon, Suresh, & Seitzman, Jerry, "Annual Report: Mechanisms of time dependent nozzle erosion processes," commissioned by the Office of Naval Research, Arlington, VA, 2005.

[2]Sutton, George P., & Biblarz, Oscar, Rocket Propulsion Elements, 7th ed., John Wiley & Sons, Inc. (2001), 605 Third Avenue, New York, NY 10158-0012.

[3]Sopok., S., Rickard, C., & Dunn, S., "Thermal-chemical-mechanical gun bore erosion of an advanced artillery system part two: modeling and predictions," WEAR, Vol. 258, 2005, p 671-683.

[4]Sopok, S., O'Hara, P., & Pflegl, G., "Unified Computer Model for Predicting Thermochemical Erosion in Gun Barrels," *Journal of Propulsion and Power*, Vol. 15, No. 4, July-August 1999, p 601-612.

[5]Niu, Yang-Yao, & Tsai, Chih-Shung, "Numerical Modeling of Erosion on the Metallic Surface by the Dilute Particulate Flow Impact," AIAA Paper 99-3761, 30th AIAA Fluid Dynamics Conference, Norfolk, VA, 1999

[6]Niu, Y., & Tsai, C., "Simulation of erosion by the dilute particle flow impact," *Numerical Heat Transfer*, Part A, Vol. 37, 2000, p 167-187.

[7]Wirzberger, H. and Yaniv, S., "Prediction of erosion in a solid rocket motor by alumina particles," 41st AIAA/ASME/ASEE Joint Propulsion Conference & Exhibit, 10-13 July, 2005, AIAA 2005-4496

[8]Palaninathan, R. & Bindu, S., "Modeling of Mechanical Ablation in Thermal Protection Systems," Journal of Spacecraft and Rockets, Vol. 42, No. 6, November-December 2005, p 971-979.

[9]Siddiqui, A. O., & Balasubrahmanyam, G., "Design of Ablative Liners for High Heat and Erosive Conditions," *Journal of Reinforced Plastics and Composites*, Vol. 24, No. 9, 2005, p 993-1007.

[10]Li, D.Y., Elalem, K., Anderson, M.J., & Chiovelli, S., "A microscale dynamical model for wear simulation," *WEAR*, Vol. 225-229, 1999, p 380-386.

[11]Elalem, K., & Li, D.Y., "Dynamical simulation of an abrasive wear process," *Journal of Computer-Aided Materials Design*, Vol. 6, 1999, p 185-193.

[12]Chen, Q., & Li, D.Y., "Computer simulation of solid particle erosion," *WEAR*, Vol. 254, 2003, p 203-210.

[13]Chen, Q., & Li, D.Y., "Computer simulation of solid-particle erosion of composite materials," *WEAR*, Vol. 255, 2003, p 78-84.

[14]Liggett, Nicholas and Menon, Suresh, "Simulation of Nozzle Erosion Process," Office of Naval Research, Arlington, VA, 2006.

[15]Snih, T. M., Numerical Heat Transfer, Hemisphere Publishing Corporation (1984), New York, NY.

[16]Tannehill, J., Anderson, D., & Pletcher, R., Computational Fluid Mechanics and Heat Transfer, 2nd ed., Taylor & Francis (1997), Philadelphia, PA 19106.

[17]Kuo, Kenneth K., Principles of Combustion, John Wiley & Sons, Inc. (1986), New York, NY

[18]Kuo, Kenneth K., & Keswani, S. T., "A Comprehensive Theoretical Model for Carbon-Carbon Composite Nozzle Recession," *Combustion Science and Technology*, Vol. 42, 1985, p 145-164.

[19]Coltrin, M.E., Kee, R.J., & Rupley, F.M., "Surface Chemkin: A general formalism and software for analyzing heterogeneous chemical kinetics at a gas-surface interface," *International Journal of Chemical Kinetics*, Vol. 23, 1991, p 1111-1128.
[20]Coltrin, M.E., Kee, R.J., & Rupley, F.M., "Surface Chemkin: A fortran package for analyzing heterogeneous chemical kinetics at a solid surface - gas phase interface," Sandia Report SAND90-8003B, July 1991.
[21]Coltrin, M.E., Kee, R.J., & Rupley, F.M., "Surface Chemkin III: User manual," *Reaction Design*, 1996.
[22]Porumbel, I. and Menon, S., "Large-Eddy Simulation of Bluff Body Stabilized Premixed Flames," AIAA-2006-0152, 44th AIAA Aerospace Sciences Meeting, Reno, NV, January, 2006.
[23]Surzhikov, S. T., & Krier, H., "Quasi-One-Dimensional Model of Combustion of Sandwich Heterogeneous Propellant," *High Temperature Mass Transfer and Physical Gas Dynamics*, Vol. 39, No. 4, 2001, p 586-595.
[24]Massa, L., Jackson, T. L., & Buckmaster, J., "New Kinetics for a Model of Heterogeneous Propellant Combustion," *Journal of Propulsion and Power*, Vol. 21, No. 5, September-October 2005, p 914-924
[25]Powers, David L., Boundary Value Problems, 4th ed., Academic Press (1999), 200 Wheeler Road, Bulington, MA 01803, USA
[26]Kuo, K.., Evans, B., Acharya, R., Favorito, N., Ferrara, P., Moore, J., & Boyd, E., "Annual Progress Report for MURI 12 Rocket Nozzle Erosion Minimization (RNEM)," commissioned by the Office of Naval Research, Arlington, VA, 2005.
[27]Yang, Vigor, & Thakre, Piyush, "Annual Report (2004/2005) Modeling and Simulation of Nozzle Material Erosion," commissioned by the Office of Naval Research, Arlington, VA, 2005.
[28]Avallone, Eugene A. & Baumeister III, Theodore, Marks' Standard Handbook for Mechanical Engineers, 10th ed., The McGraw-Hill Companies, Inc. (1996), New York, NY.
[29]Lee, Tae-Ho, "Experimental Study of the Nozzle Surface Regression Rate to the Heat Transfer," *Journal of Propulsion and Power*, Vol. 22, No. 1, January-February 2006, p 221-223.
[30]Gowariker, V. R., "Mechanical and Chemical Contributions of the Erosion Rates of Graphite Throats in Rocket Motor Nozles," *Journal of Spacecraft and Rockets*, Vol. 3, No. 10, October 1966, p 1490-1494.
[31]Gates, A. M, "In situ measurements of carbon dioxide, 0.37–4.0 μm particles, and water vapor in the stratospheric plumes of small rockets," *Journal of Geophysical Research* (2002), Vol. 107, No. D22, p AAC8-1-10.

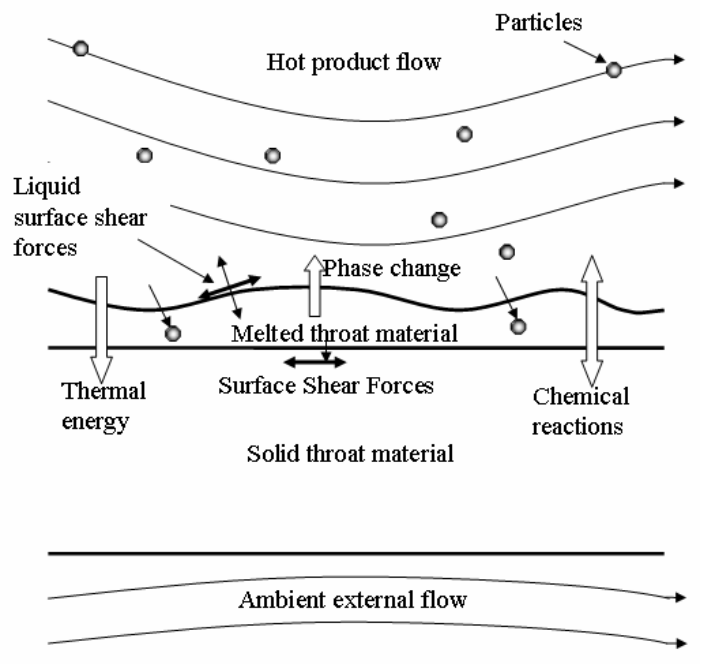

Figure 1. Physical processes affecting erosion.

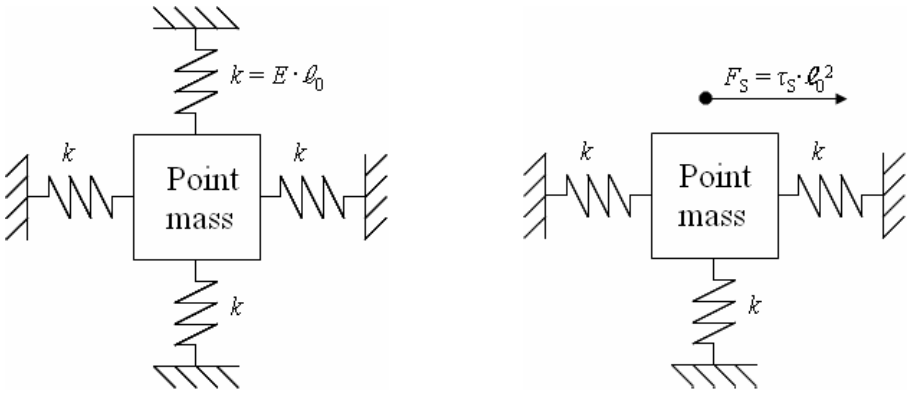

(a) Interior site **(b) Exposed site**

Figure 2. Lattice site for MSD model.

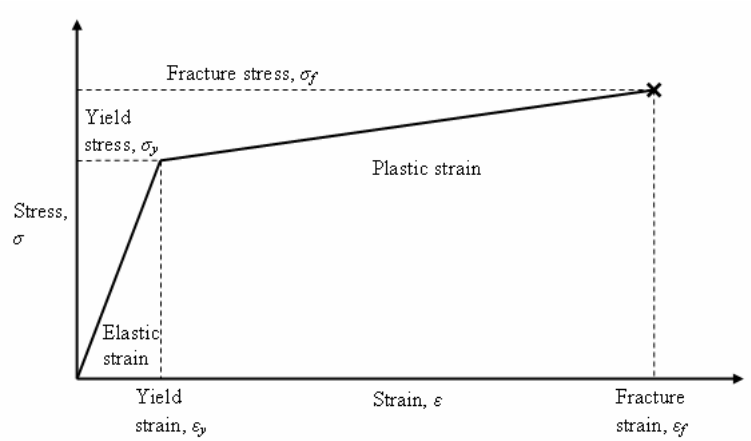

Figure 3. Stress-strain curve demonstrating elastic and plastic regimes.

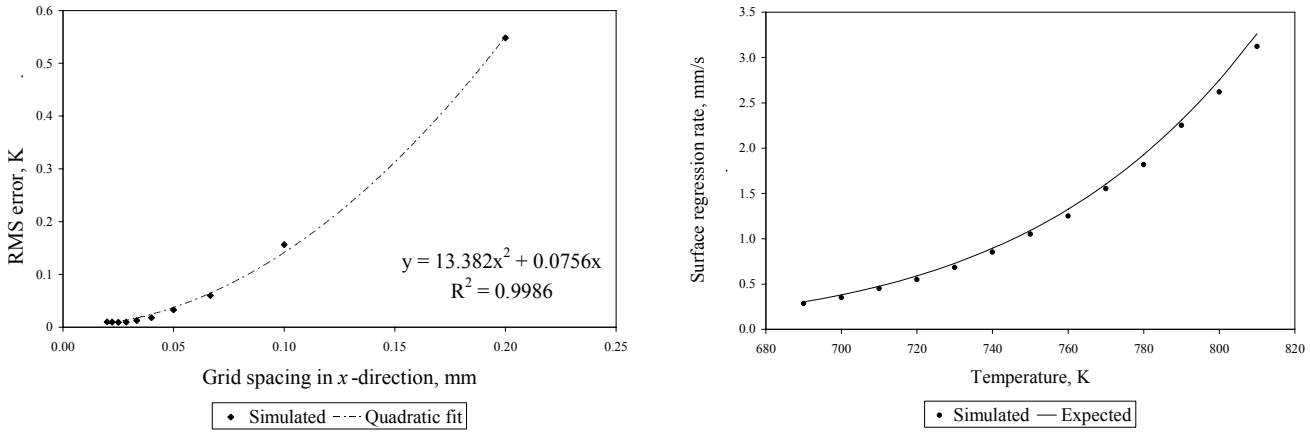

(a) RMS error for thermal model **(b) AP surface regression rates**

Figure 4. Simulation and validation data for model validation.

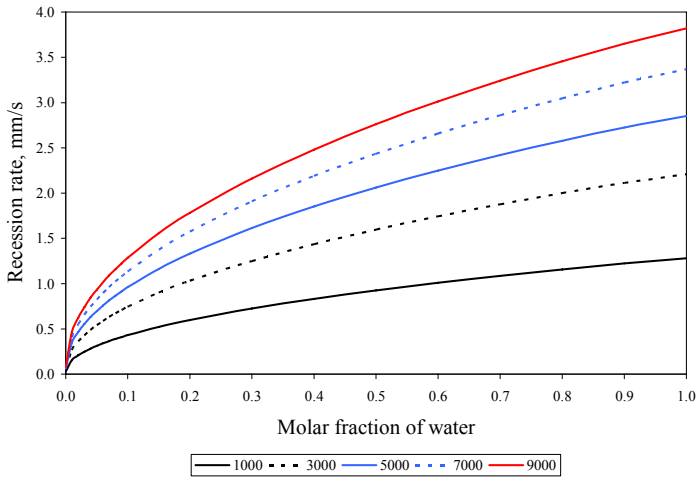

Figure 5. Recession rate of carbon nozzle with varying chamber pressures, psi.

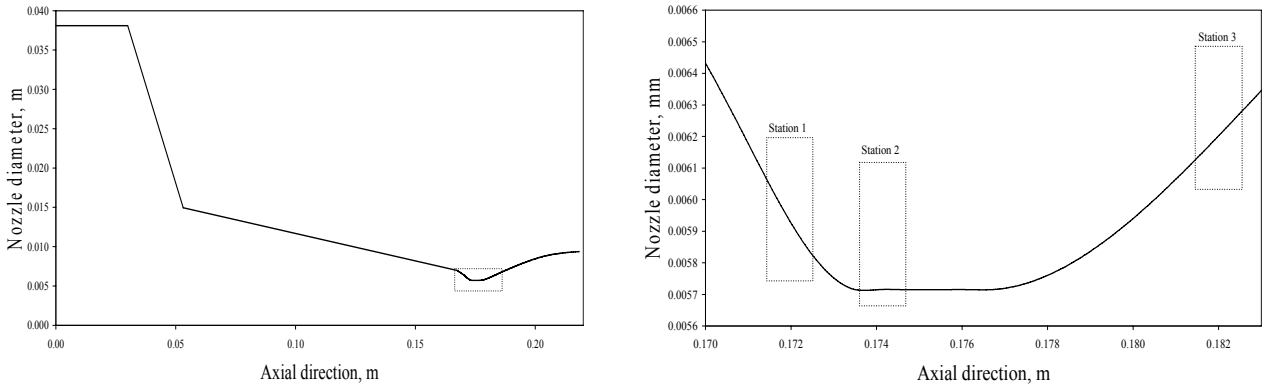

(a) Gross nozzle geometry **(b) Profiles for stations**

Figure 6. Nozzle geometry used for erosion studies.

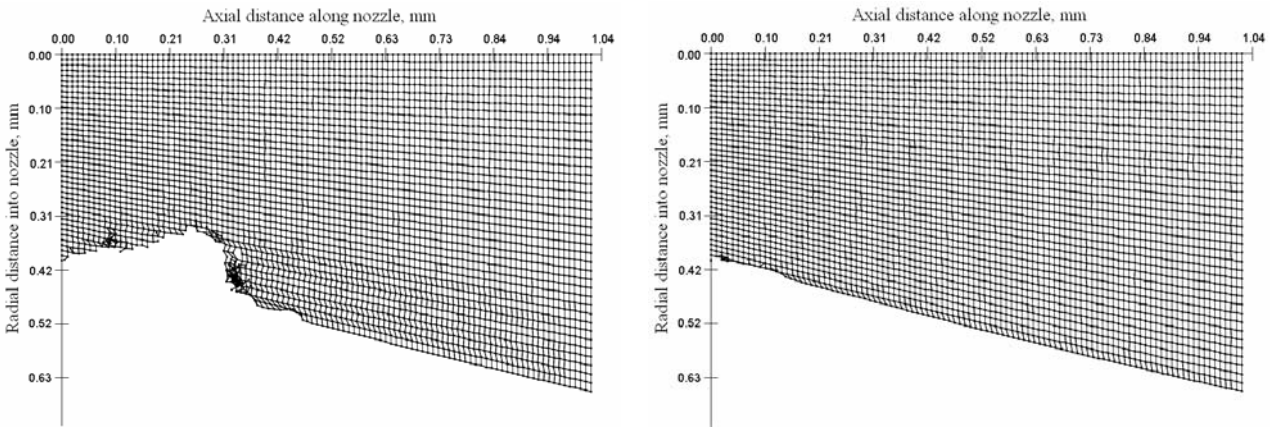

(a) Niobium **(b) Tungsten-rhenium**

Figure 7. Particle impact simulation results at station 1, before the throat.

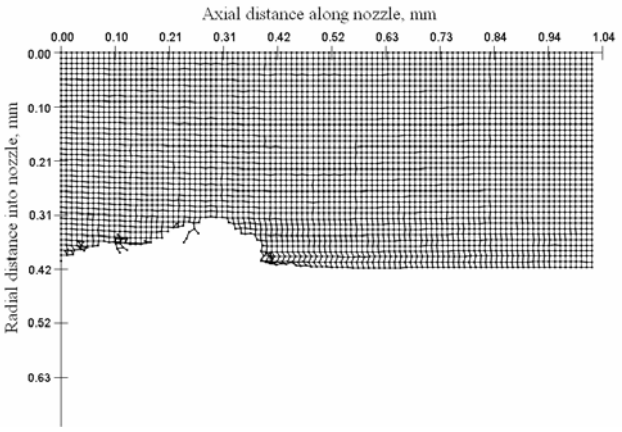

(a) Niobium

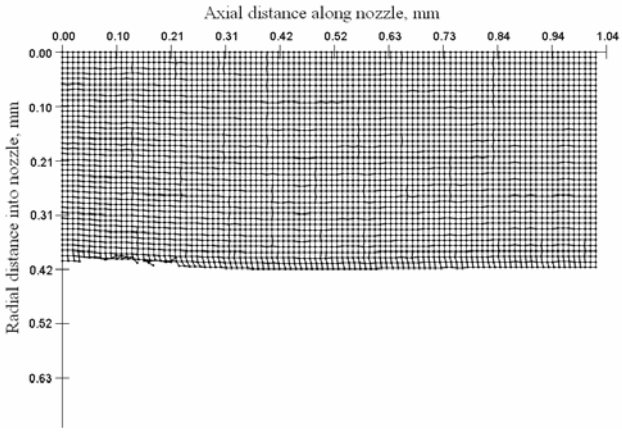

(b) Tungsten-rhenium

Figure 8. Particle impact simulation results at station 2, at the throat.

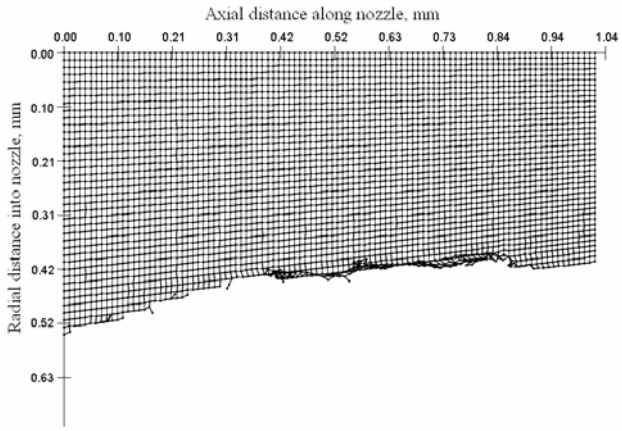

(a) Niobium

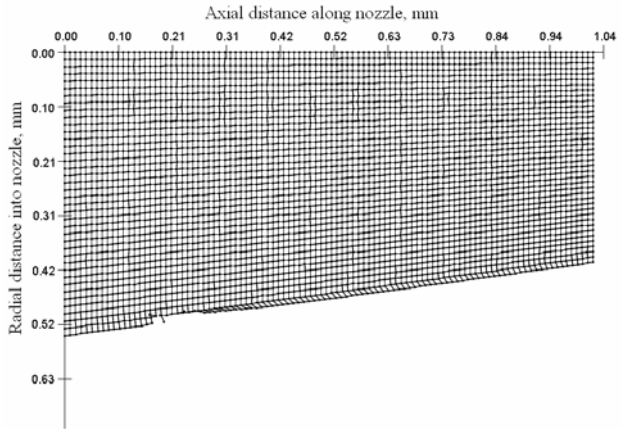

(b) Tungsten-rhenium

Figure 9. Particle impact simulation results at station 3, after the throat.

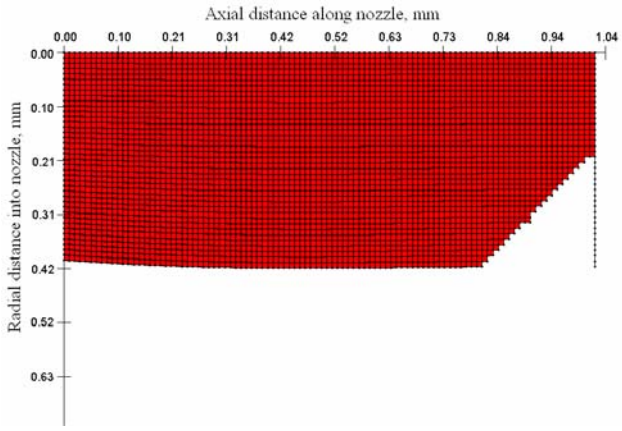

(a) Niobium

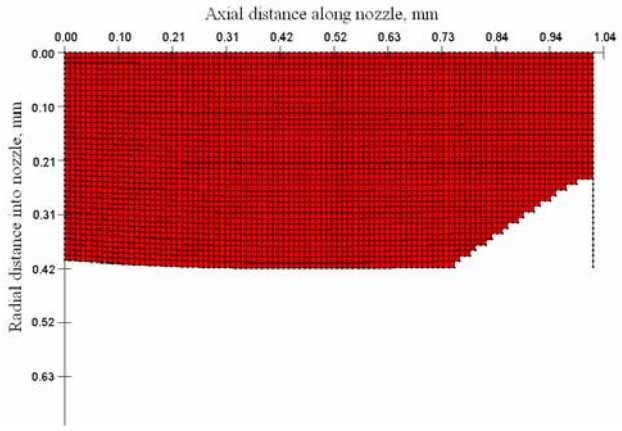

(b) Tungsten-rhenium

Figure 10. Heat transfer simulation results at station 2, at the throat.